Applied Surface Science 440 (2018) 266–274

Contents lists available at ScienceDirect

Applied Surface Science

journal homepage: www.elsevier.com/locate/apsusc

Full Length Article

Visible-Light Upconversion Carbon Quantum Dots Decorated TiO_2 for the Photodegradation of Flowing Gaseous Acetaldehyde

Yidan Hu [a,b], Xiaofeng Xie [a,*], Xiao Wang [a], Yan Wang [a], Yi Zeng [a], David Y.H. Pui [c], Jing Sun [a]

[a] Shanghai Institute of Ceramics, Chinese Academy of Sciences, 1295 Dingxi Road, Shanghai 200050, China
[b] University of Chinese Academy of Sciences, 19 (A) Yuquan Road, Beijing 100049, China
[c] College of Science and Engineering, University of Minnesota, Minneapolis, MN 55455, USA

ARTICLE INFO

Article history:
Received 10 December 2017
Revised 5 January 2018
Accepted 10 January 2018
Available online 31 January 2018

Keywords:
Carbon quantum dots
Titania
Upconversion
Photocatalysis
Acetaldehyde removal

ABSTRACT

Carbon-modified photocatalyst has attracted extensive attentions in the field of gaseous pollutant removal, mainly due to the improved adsorption properties and electronic transport of carbon matrix, such as carbon nanotubes, graphene, and fullerene, etc. In this work, carbon quantum dots (CQDs) were employed to enhance the photocatalytic performance of TiO_2-based composites for flowing gaseous acetaldehyde removal. Besides the aforementioned advantages of carbon materials, the unique up-converted photoluminescence property of CQDs is capable of extending the optical absorption to visible-light range. Moreover, the electron spin resonance (ESR) results firstly verified a stable existence of Ti^{3+} defect in the CQDs/TiO_2 composite, which is possibly induced by the electron migration from CQDs to TiO_2. And the formed Ti^{3+} donor energy level in the band gap could further help with the visible-light harvesting. During the photodegradation experiments, with two-hour continuous flowing gaseous acetaldehyde injection (500 ppm, 20 sccm), the CQDs/TiO_2 composite remained 99% removal efficiency under fluorescent lamp irradiation ($\lambda > 380$ nm). The optimized CQDs content was obtained as 3 wt%, and the underlying mechanism was further analyzed by temperature programmed desorption (TPD) methods. This work will push forward the air purification researches by providing new insights of CQDs sensitized photocatalyst.

1. Introduction

Volatile organic compounds (VOCs) are the dominating indoor contaminates that can be released from cooking fuels, house furnishings, or any chemical involved material [1]. As it is reported that time-weighted exposure to indoor pollutants may cause high rates of morbidity and mortality, the indoor air quality is rather important to human's health [2–4]. A notorious example is acetaldehyde, which is usually accompanied with the oxidation of unsaturated fatty acids or the cleavage of photoinitiators under light, or even the hydrolysis of some composite building materials containing esters [5]. With a highly reactive nature, acetaldehyde not only directly threatens human's health due to its cytotoxicity, mutagenicity, and carcinogenicity, but also readily participates in rearrangement of chemical compounds through further reacting with O_3, NO*x* and other reactive gases [5,6].

In the latest, photocatalytic oxidation (PCO) technology has been progressively applied in indoor air purification, due to its room-temperature feasibility, environmental friendliness and chemical activity toward most of contaminates [7–9]. Through the PCO process, most organic molecules could be photodegraded into smaller benign products such as CO_2 and H_2O. Various photocatalysts have been investigated and applied into PCO field, among which TiO_2 photocatalyst has been most widely studied, owing to its comprehensive properties of good chemical stability, superior photocatalytic oxidation ability and outstanding biocompatibility [10]. However, with relatively broad band gap (~3.2 eV), TiO_2 photocatalyst can only be activated by ultraviolet light. Besides, the high electron-hole recombination efficiency of TiO_2 also confines the photocatalytic behavior. Many efforts hitherto have been made to ameliorate the photocatalytic ability, including metal [11] or non-metal [12] ion doping, dye-sensitization [13,14], heterojunction with narrow-bandgap semiconductors [15,16] or noble metals [17–19].

Recently, carbon quantum dots (CQDs) has been identified to sensitize some semiconductors, such as TiO_2 [20], g-C_3N_4 [21], Bi_2S_3 [22], CdS [23], for enhancing optical responsiveness and photocatalytic performance. Compared with graphene [24], carbon nanotube [25] and fullerene [26,27], the zero-dimensional CQDs

* Corresponding author.
E-mail address: xxfshcn@163.com (X. Xie).

https://doi.org/10.1016/j.apsusc.2018.01.104
0169-4332/

possess some unique and superior optical and electron properties [28], such as excellent light-harvesting, tunable photoluminescence and efficient electron-trapping ability. Especially, CQDs are confirmed to have the extraordinary up-converted photoluminescence (UCPL) property, capable of transferring low-energy light to high-energy light via the multiple photon-absorption of CQDs [29]. Up to now, most the reports of CQDs-based TiO_2 composites concentrate on the study of water-phased photocatalytic process, such as photo-degradation of organic dyes (e.g. methyl blue and RhB), and photocatalytic water splitting [29–32]. However, the photocatalytic effect of CQDs/TiO_2 composites involved the oxidation of gaseous pollutants has been rarely investigated, particularly for these flowing gaseous organic compounds. Both of CQDs and TiO_2 are easily attainable and nontoxic, and thus it is of theoretical and practicable favor to construct CQDs/TiO_2 composite photocatalyst for enhancing the visible-light-driven photocatalytic ability and apply it into the indoor air purification.

Herein, we synthesized CQDs/TiO_2 composites through a facile method. The photocatalytic performance and mechanism of decomposing flowing gaseous acetaldehyde were investigated. After decorating with CQDs, the modified TiO_2 photocatalyst shows an enhanced photodegradation ability under visible light irradiation and suggests a good application in indoor air purification. Additionally, a favorable defect of Ti^{3+} has been unexpectedly detected in the TiO_2 matrix after CQDs modification, which not only demonstrates an interfaced electron migration and also further enhances the visible-light photocatalysis.

2. Experimental section

2.1. Synthesis of CQDs/TiO_2 photocatalysts

All reagents, including commercial TiO_2 powder (P25), urea and citric acid (AR, Sinopharm Chemical Reagent Corp, China) were used as received without any further purification.

CQDs synthesis involves a hydrothermal method based on a previous report [33]. Briefly, 1.0 g urea and 1.0 g citric acid were dissolved in 15 ml ultrapure water and then the mixture was transferred into 30 ml Teflon autoclave at 180 °C for 6 h. After cooling down to room temperature, the product (dark green solution), was centrifugated at 12,000 rpm for 20 min to remove the large particles. The remaining solvent was dried at 80 °C for 10 h to obtain black CQDs solid.

CQDs/TiO_2 composite photocatalysts were prepared according to previous report [29]. P25 was ultrasonically dispersed into 20 ml ethanol, and the CQDs was dissolved into 15 ml ultrapure water. Then, the CQDs solution was dropwise added into the stirring P25 suspension, and the mixture stirred to be dried. The obtained solid mixture was calcined at 300 °C for 3 h in the muffle furnace. Then, the substance was washed with ultrapure water and ethanol for several times, and dried for 24 h at room temperature to obtain the CQDs/TiO_2 composites. The collected CQDs/TiO_2 products were named as *x* wt% CQDs/TiO_2, where *x* = 1, 3, 7, represent the mass percentage of CQDs to TiO_2 in the composites.

2.2. Characterizations

The morphology and crystallography of the samples were investigated by high-resolution transmission electron microscopy (HTEM, JEM-2100F). The crystal structures of the samples were characterized by X-ray diffractometer (XRD, Rigaku D/Max 2200PC) with Cu Kα radiation. Fourier transform infrared (FTIR) spectra were measured by a Thermal Scientific 5225 Verona Rd with the KBr pellet technique. X-ray photoelectron spectroscopy (XPS) data were recorded by a Thermal Scientific ESCALAB-250 using Al Kα radiation line source and the binding energies were calibrated by setting O 1s peak of pristine TiO_2 to 530.26 eV. Diffuse reflectance ultraviolet–visible (UV–vis) spectra were obtained on a Shimadzu UV-3600 spectrometer by using $BaSO_4$ as reference. Photoluminescence (PL) spectra of the samples were examined at room temperature by an Edinburgh Instruments FLSP-920 fluorescence spectrophotometer with an excitation wavelength of 320 nm.

Electron spin resonance (ESR) signals of reactive species spin-trapped by 5,5-dimethyl-L-pyrroline-N-oxide (DMPO) were determined on a JES-FA200 spectrometer. Photocatalysts were dispersed in DMPO/ethanol solution and DMPO/H_2O solution for detection of superoxide radicals ($\cdot O_2^-$) and hydroxyl radicals (**.**OH), respectively. A 500 W xenon lamp was used as the irradiation source.

2.3. Photocatalytic activity measurements

The photocatalytic performance of CQDs/TiO_2 composites for flowing gaseous acetaldehyde degradation was conducted in a reactor chamber which was a 300 cm^3 cuboid quartz vessel (20 cm × 10 cm × 1.5 cm) with an inlet and an outlet for gas flow. This chamber is connected to an online photocatalysis test system combining with gas chromatograph (SP 502, high purity nitrogen as carrier gas), to detect the flowing acetaldehyde concentration. All the photocatalytic experiments were carried out at room temperature, using a fan cooling system to maintain the thermal condition, and the relative humidity was kept at ~45%.

The photocatalytic experimental samples were prepared through a coating method. In brief, 0.1 g photocatalyst was ultrasonically dispersed in ethanol, and the slurry was homogeneously coated onto a glass plate to form a thin film (6 cm × 13 cm). After being dried, the tested sample was transferred into the reactor chamber, and gaseous acetaldehyde (500 ppm) mixed with air flowed into the chamber at 20 sccm flow rate. The photocatalytic experiments contained the following steps: first, the photocatalyst fully adsorbed acetaldehyde to reach an adsorption/desorption equilibrium in the dark condition (the GC detection showed a renatured concentration of acetaldehyde); second, with light irradiation, the gaseous acetaldehyde continuously flowed through the reactor chamber and the concentration was measured by GC with 5 min intervals. Household fluorescent lamps (4 × 65 W, λ > 380 nm) and a xenon lamp with UV-cut filter (λ > 400 nm) were used as the irradiation sources in the photocatalytic process. The efficiency for photo-decomposing acetaldehyde was calculated as follows:

$$\eta = \frac{C_0 - C}{C_0} \times 100\%$$

where C_0 presents the original acetaldehyde concentration after it reaching an adsorption/desorption equilibrium on photocatalysts, and C is the real-time acetaldehyde concentration detected during the photodegradation process.

2.4. Photoelectrochemical measurements

The photoelectochemical measurements of CQDs/TiO_2 were performed on a CHI 660A electrochemical workstation (Chenhua Instrument, Inc.). Three-electrode system consisting of platinum wire as counter electrode, Ag/AgCl in saturated KCl as reference electrode and sample-coated fluorine-doped tin oxide substrate (FTO) as working electrode was used for the measurement. 1 M NaCl solution was used as electrolyte. The working electrode was prepared as follows: 100 mg sample was ultrasonically dispersed into 2.0 g ethanol for 1 h, then 300 μL slurry was spin-coated at 1000 rpm for 20 s to form a 1 cm × 2.5 cm sample film onto the FTO substrate. Finally, the FTO substrate with sample film was

dried at 80 °C for 30 min. A xenon lamp with UV-cut filter (λ > 400 nm) was used as the irradiation source in the photocurrent test.

2.5. Acetaldehyde-TPD measurements

The acetaldehyde temperature-programmed desorption (acetaldehyde-TPD) measurements were carried out by PCA-1200 equipped with a thermal conductivity detector. For acetaldehyde-TPD, 400 mg sample was soaked in N_2 flow at 120 °C for 1 h first, and then cooled to 30 °C and adsorbed flowing gaseous acetaldehyde for 2 h. After purging with N_2 for 10 min to remove the unadsorbed acetaldehyde in the pipeline, the sample in N_2 flow was heated at the rate of 10 °C min^{-1} to obtain the acetaldehyde-TPD profile.

3. Results and discussion

3.1. Characterizations of CQDs/TiO_2

In this experiment, CQDs with averaged size of 4–5 nm has been successfully synthesized, which owned a well-crystallized core and an amorphous shell as revealed in the HRTEM image (Fig. S1). Notably, in the up-converted photoluminescence spectra (Fig. S2), with the excitation wavelength ranging from 600 nm to 800 nm, the CQDs can irradiate up-converted emissions located in the range of 375–550 nm, which suggests that the synthesized CQDs could desirably convert those visible or near-infrared light to short-wavelength light with higher photon energy.

According to the overall TEM image of CQDs/TiO_2 composites in Fig. 1a, it reveals a coupling structure that several monodispersed CQDs (4–5 nm in diameter) attach to the surface of TiO_2 particles, which are 20–30 nm in diameter. As shown in Fig. 1b, the interplanar spacing of 0.249 nm and 0.187 nm belong to the (1 0 1) plane of rutile TiO_2 and the (2 0 0) plane of anatase TiO_2, respectively (JCPDS card no. 21-1276 and no. 21-1272), while the interplanar spacing of 0.217 nm is assigned to the (0 0 1) plane of graphene carbon. And that demonstrates the successful coupling of CQDs with TiO_2. To further confirm the CQDs are well decorated on TiO_2, the FTIR spectra (Fig. 1c) of CQDs/TiO_2 were carried out. Compared with the pristine TiO_2, some new functional groups can be observed in CQDs-modified TiO_2. The typical absorption peaks at 1635 cm^{-1} and 3420 cm^{-1} are assigned to the vibration of water absorbed on the surface of substance. The new appeared peaks in CQDs/TiO_2 composite at 2974 cm^{-1} (CH_2), 1226 cm^{-1} (CH), 1157 cm^{-1} (C═O) are ascribed to the addition of CQDs [29], evidently confirming the existence of CQDs in the CQDs/TiO_2 composites. Although the XRD patterns only show the characteristic diffraction line of anatase and rutile phases belonging to TiO_2 (Fig. 1d), the existence of CQDs cannot be ignored, which is resulted from very slight amount of CQDs in the composites.

Subsequently, XPS was employed to further investigate the interaction between CQDs and TiO_2. The full survey spectrum of the CQDs/TiO_2 composite, indicating the presence of titanium (Ti 2p), carbon (C 1s) and oxygen (O 1s), is showed in Fig. 2a. In Fig. 2b, two fitted peaks of 3 wt% CQDs/TiO_2 composite located at 459.3 and 464.91 eV could match with the Ti $2p_{3/2}$ and Ti $2p_{1/2}$ of TiO_2 [34,35], the subdued binding energy compared with pristine TiO_2 implying that the chemical environment of Ti has changed after combining with CQDs. In the C 1s spectrum (Fig. 2c), the dominated peak referring to C—C bond with sp^2 orbital mainly belongs to surface carbon contaminate [36], and the peak shifts from 287.14 eV to 285.65 eV after cooperating with CQDs. Due to the different carbon's chemical valence state between electroneutral CQDs and surface carbon contaminate with positive charged

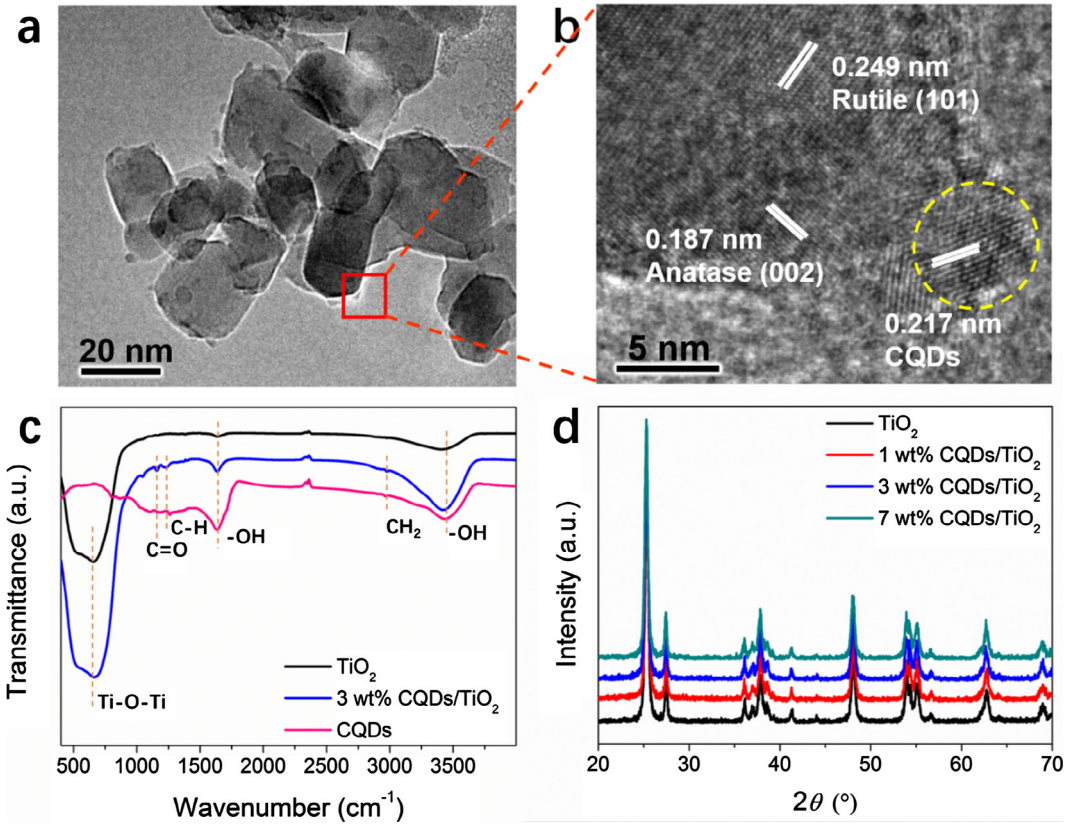

Fig. 1. Morphological and structure characterizations of CQDs/TiO_2 composites. (a) Overall TEM image of 3 wt% CQDs/TiO_2 sample. (b) Zoom-in HRTEM image of the marked region in (a). (c) FTIR spectra of pristine TiO_2, 3 wt% CQDs/TiO_2 and CQDs sample. (d) XRD patterns of CQDs/TiO_2 composites with different CQDs content.

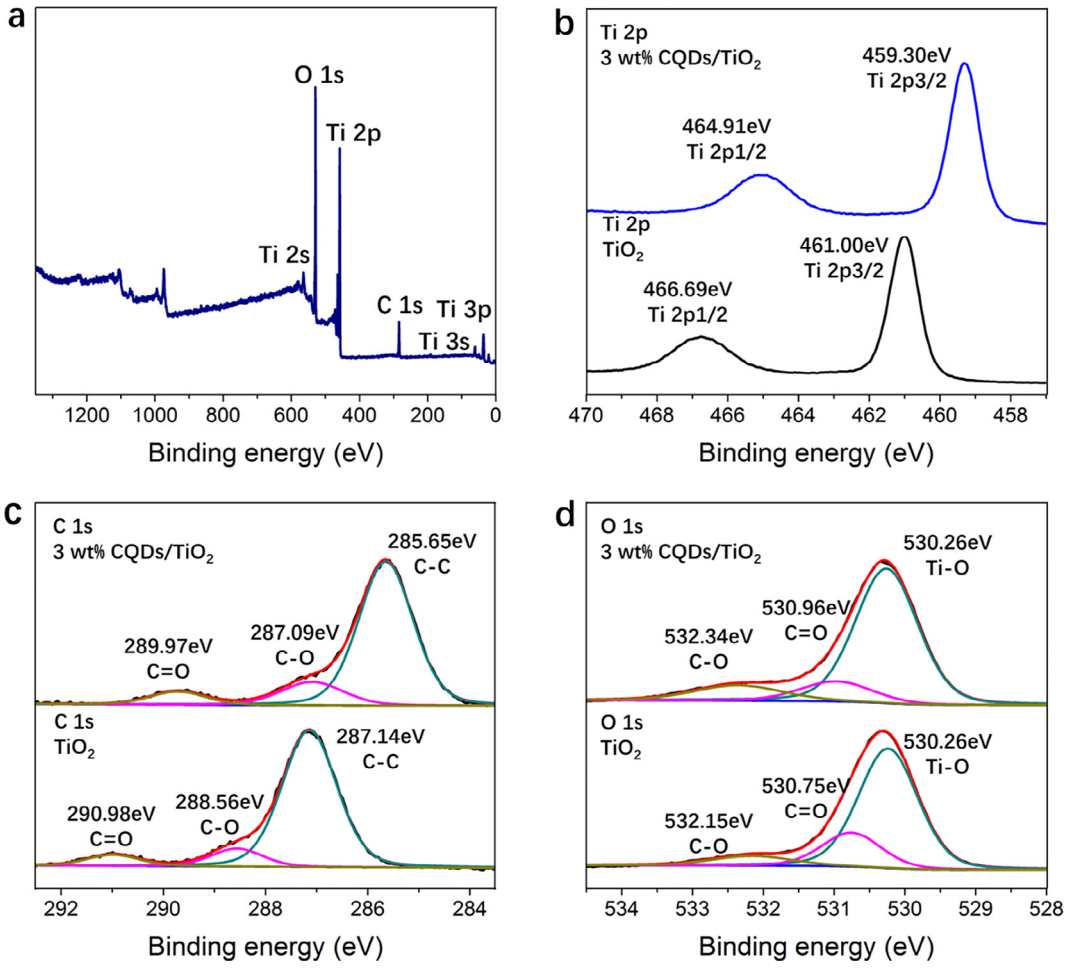

Fig. 2. (a) XPS survey spectrum of 3 wt% CQDs/TiO_2 composite. (b–d) Corresponding high resolution XPS spectra of Ti 2p (b), C 1s (c), O 1s (d) of TiO_2 and 3 wt% CQDs/TiO_2 composite.

carbon, it is reasonable after adding CQDs the binding energy of C—C bond reduced. Additionally, No peak corresponding to Ti—C bond at around 281 eV was observed [37], suggesting that the carbon does not dope in and distort the TiO_2 phase. However, it is found that the binding energy of Ti—O and C—O are weakened, which could infer that the CQDs are grafted onto the surface of TiO_2 via Ti—O—C bond. Besides, the reduced binding energy of Ti 2p (Fig. 2b) in 3 wt% CQDs/TiO_2 composite could suggest an electron-migration occurrence between TiO_2 and CQDs.

Since the XPS measurement merely analyzed the surface chemical state within a few nanometers in depth, ESR spectroscopy which enables an overall detection of the material was employed to further investigate the electron-migration phenomenon. Surprisingly, Ti^{3+} defect (g = 1.98) [38] are detected in CQDs/TiO_2 samples while no such signal presents in pristine TiO_2 (Fig. 3a), and the Ti^{3+} signals strengthen positively with the addition of CQDs. Since it is hard for Ti^{4+} ion reduction happening during such mild and aerobic synthesized process [39], the existence of Ti^{3+} defect could possibly originate from the different electron work function between CQDs and TiO_2. Due to special electron structure, the work function of CQDs might be lower than that of TiO_2, resulting in delocalized electron migration from CQDs to TiO_2, which makes the TiO_2 be negatively charged and form Ti^{3+} defect, similar to the electron interaction between metal and semiconductor [40,41].

Viewing the result of UV–vis absorption spectra (Fig. 3b), CQDs/TiO_2 composites show an enhanced optical absorption in visible region compared with pristine TiO_2, and the absorption increases gradually with the CQDs addition, ascribed to the UCPL property [42]. Moreover, the absorption edges of modified TiO_2 also slightly red-shift, from ~400 nm to ~420 nm, suggesting the band gaps of composite photocatalysts narrow down after conjoining CQDs and the optical response correspondingly expand. Based on the aforementioned ESR results of CQDs/TiO_2 composites, the decreased band gaps of modified TiO_2 could result from the existence of Ti^{3+} ion, which is capable of generating a defective energy level under conduction band [38].

3.2. Photocatalytic degradation of acetaldehyde

The photocatalytic ability for decomposing gaseous acetaldehyde via pristine TiO_2 and CQDs/TiO_2 composite samples were evaluated under the irradiation of household fluorescent lamp ($\lambda > 380$ nm, 20 mW cm^{-2}) and visible light ($\lambda > 400$ nm), respectively.

As shown in Fig. 4a, in the flowing gaseous acetaldehyde (500 ppm, 20 sccm), all CQDs/TiO_2 composite samples present an enhanced photocatalytic property over pristine TiO_2. After two-hour light irradiation, the pristine TiO_2 sample removes acetaldehyde by 46% and CQDs show no photocatalytic activity, while the highest degradation efficiency 99% can be achieved in 3 wt% CQDs/TiO_2 composite, of which the efficiency is two times as high as that of pristine TiO_2. It is worth mentioning is that since the gaseous acetaldehyde is continuously flowing into reactor chamber, it is reasonable for acetaldehyde not being thoroughly eliminated. As can be seen from the less acetaldehyde removal efficiency of 1 wt%

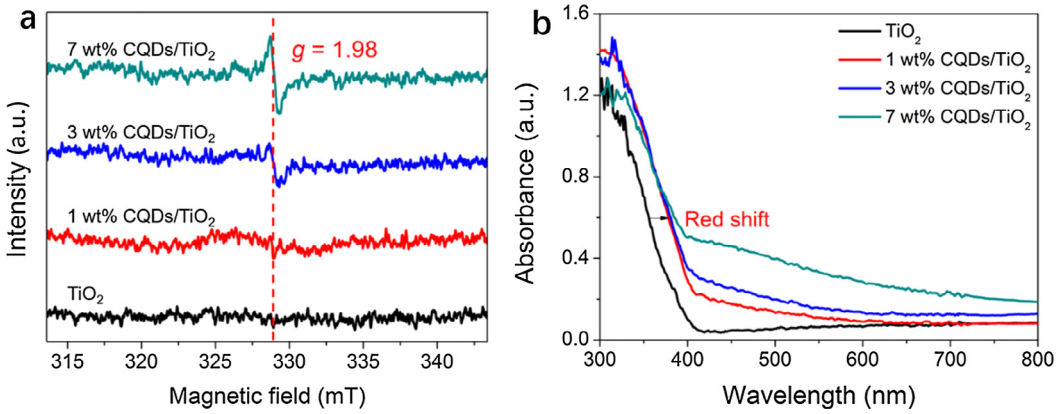

Fig. 3. (a) Electron spin resonance (ESR) spectra at room temperature and (b) Diffuse reflectance UV–vis spectra of CQDs/TiO_2 composites with different CQDs content.

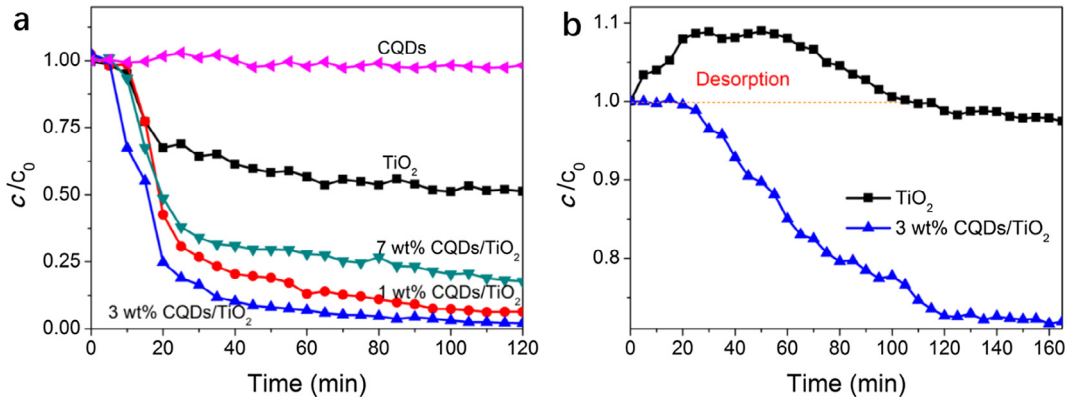

Fig. 4. Photocatalytic degradation of flowing gaseous acetaldehyde (500 ppm, 20 sccm) by CQDs/TiO_2 composites with different CQDs content under (a) fluorescent lamp irradiation (λ > 380 nm, 20 mW cm^{-2}) and (b) visible light irradiation (λ > 400 nm).

and 7 wt% CQDs/TiO_2 composites in Fig. 4a, further more or less addition of CQDs in composites could induce a relatively less improved photocatalytic performance, suggesting that a suitable amount of CQDs could effectively refine the TiO_2. Under the visible light irradiation (as shown in Fig. 4b), the 3 wt% CQDs/TiO_2 composite sample can eliminate 30% acetaldehyde, while the pristine TiO_2 shows an incapable photocatalytic performance (after light on, some previous absorbed acetaldehyde on TiO_2 surface desorbs due to the increased temperature by the significant heat effect under irradiation).

3.3. Adsorption of gaseous acetaldehyde

To investigate the reason for varied amounts of CQDs differently influencing the photocatalytic activity, the adsorbability for acetaldehyde via photocatalysts was then studied. The temperature programmed desorption (TPD) measurement result of pristine TiO_2 and 3 wt% CQDs/TiO_2 is reported in Fig. 5a, where the integral area of peak is corresponding with the amount of desorbed acetaldehyde and its further products during the thermal annealing process. The first peak at 110–120 °C is ascribed to the desorption of water and physically adsorbed acetaldehyde. The second peak, at around 200 °C could be involved with the products of acetaldehyde's aldol condensation on the photocatalyst surface, for example, crotonaldehyde ($CH_3CH{=}CHCHO$), crotyl alcohol ($CH_3CH{=}CHCH_2OH$), and the third peak at 325–340 °C could be assigned to some olefins [43]. Viewing the spectra coverage, the total amount of desorbed substance of 3 wt% CQDs/TiO_2 composite is more than that of pristine TiO_2, so it can be inferred that the coupled CQDs could help with the adsorption of acetaldehyde, further assisting the photocatalytic process.

Additionally, the dynamic adsorption in the reactor chamber for flowing acetaldehyde gas upon all samples were tested and calculated (seeing Fig. 5b). The result of adsorption calculation indicates that the adsorption for acetaldehyde is positively correlated with the amounts of CQDs in the composites, which further supports the result of TPD measurement. And due to the contribution of CQDs, the improved adsorbability for acetaldehyde could be one of the reasons for enhanced photocatalytic property among all CQDs/TiO_2 composites. However, although more CQDs loaded on TiO_2 could help to promote the adsorption of acetaldehyde, superfluous acetaldehyde accumulation on photocatalyst surface might suppress the substance migration and the active sites of TiO_2 surface also would be covered by overloaded CQDs, both of which would result in a hindrance of photocatalytic process.

3.4. Photo-generated carrier recombination

The photoluminescence (PL) spectra of pristine TiO_2 and CQDs/TiO_2 composites are showed in Fig. 5c. Under 320 nm excitation at room temperature, all samples present a broad PL emission with a cascade of several peaks, located in 380–480 nm. Reasonably, it is the heterostructured nature consisted of anatase and rutile in the P25 that bring about the complexed PL emissions of which the photon energies are equal to band gaps of semiconductor. Taking all the emission spectrums in comparison, it is highlighted that the PL intensity decreases with raised CQDs concentration in CQDs/TiO_2. In pristine TiO_2, the photo-generated electrons which

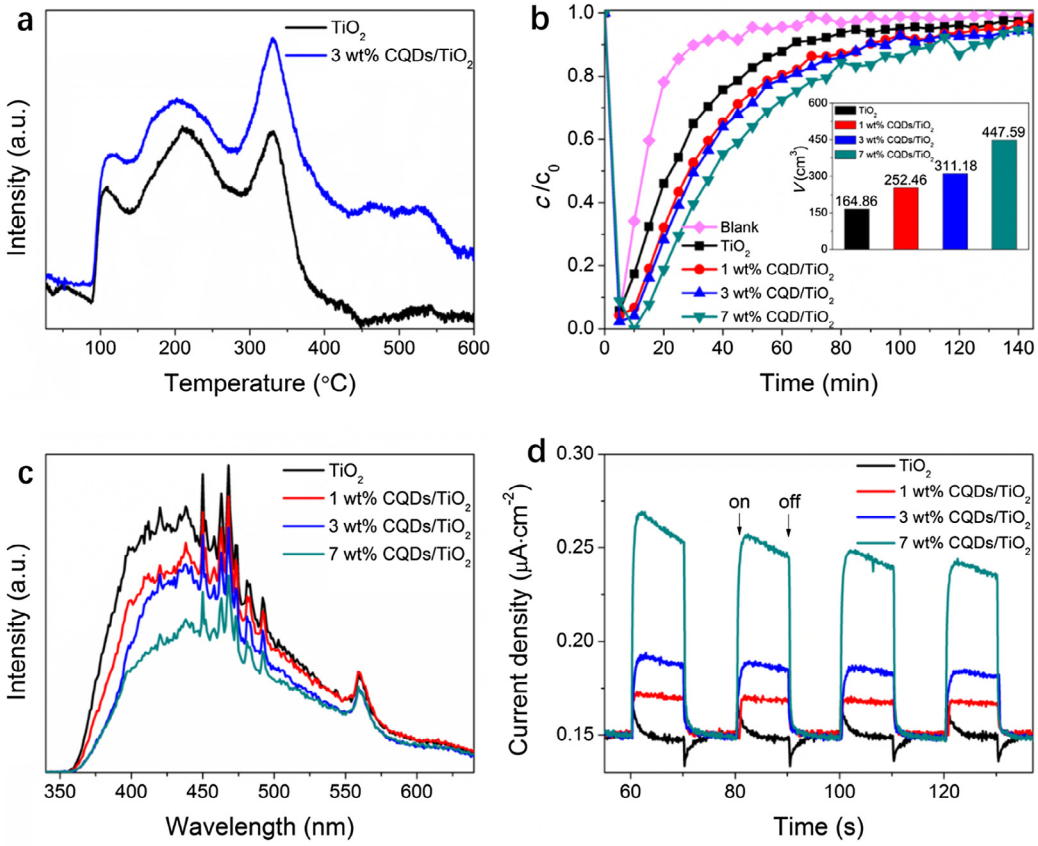

Fig. 5. (a) Temperature programmed desorption (TPD) spectra of acetaldehyde upon pristine TiO_2 and 3 wt% CQD/TiO_2 composite. (b) Dynamic acetaldehyde adsorption process for 140 min without illumination and related absorbance calculation over different samples and none sample (blank) in the reactor chamber. (c) Photoluminescence spectra (PL) of CQDs/TiO_2 composites with different CQDs content at an excitation wavelength of 320 nm. (d) Periodic photocurrent responses of CQDs/TiO_2 composites with different CQDs addition under visible-light irradiation ($\lambda > 400$ nm).

are excited by photons transfer from exited state to ground state and recombine with holes, following by emission of fluorescence. While in CQDs/TiO_2 samples, the CQDs could serve as qualified electron reservoirs, and the photo-generated electrons on the conduction band of TiO_2 are inclined to migrate to CQDs. Therefore, under the influence of CQDs, the recombination of photo-generated electrons and holes could be effectively obstructed, which will benefit the photocatalytic process.

The photo-electrochemical experiment was carried out to investigate the photoinduced charge-transfer behavior. According to Fig. 5d, under visible light ($\lambda > 400$ nm) irradiation, all CQDs/TiO_2 samples show noticeable photocurrent responses while the pristine TiO_2 only has a very small photocurrent signal during several on-off cycles of irradiation. This phenomenon further proves that the modified TiO_2 could be activated under visible-light irradiation with the sensitization effect of CQDs, of which the result is rationally in accordance with the improved photodegradation behavior for acetaldehyde upon CQDs/TiO_2 (Fig. 4). Besides, the changing trend of photocurrent intensity is positively correlated with the mass of CQDs in composites. It suggests that CQDs play a significant role in the separation/transfer process of photo-generated charge carriers, resulting in a lowered recombination rate of photo-generated electron-hole pairs, which are in line with the PL result illustrated in Fig. 5c.

3.5. DMPO spin-trapping ESR spectra

Generally, the PCO process involves several reactive oxygen species, such as superoxide radical ($\cdot O_2^-$), hydroxyl radicals ($\cdot OH$) and hydrogen peroxide (H_2O_2), which play a vital role in the PCO process [44]. The ESR spin trapping technique was applied to investigate the radical species formed under xenon lamp irradiation of pristine TiO_2 and 3 wt% CQDs/TiO_2 composite, as shown in Fig. 6. It could be observed that after 5 min irradiation, pristine TiO_2 and CQDs/TiO_2 composite samples produce the typical radical intermediates. In the spectra, the four-line ESR signals with intensity ratios of 1: 1: 1: 1 and 1: 2: 2: 1 are respectively classified to the characteristic signals of DMPO- $\cdot O_2^-$ and DMPO- $\cdot OH$ adducts [45]. It is noticeable that the DMPO- $\cdot O_2^-$ signals of the composites are much stronger than that of pristine TiO_2 in the same irradiative condition, and the 3 wt% CQDs/TiO_2 sample yields the most $\cdot O_2^-$ species. The reasons for enhanced $\cdot O_2^-$ production upon CQDs/TiO_2 composites could be explained as follows: (a) Due to the high electron affinity of dioxygen [46,47], the created Ti^{3+} defects with negative charge in the TiO_2 photocatalyst favor free O_2 adsorption. (b) Under the light irradiation, as the photo-generated electrons transfer to CQDs which also turns to be negatively charged, the suppressed electron-hole recombination induces more photo-generated electron to generate $\cdot O_2^-$ radicals. However, excessive CQDs covered on TiO_2 might prohibit the photocatalytic activity and generate less charge carriers, matching with the consequence of above photodegradation test (Fig. 4a). Besides, judging from Fig. 6b, it indicates that introducing more CQDs to the composites would cause a negative effect on the formation of $\cdot OH$. Taken together, loading CQDs on TiO_2 surface benefits the $\cdot O_2^-$ yield, which constitutes the dominated oxygen reactive species during the PCO process of CQDs/TiO_2 photocatalyst.

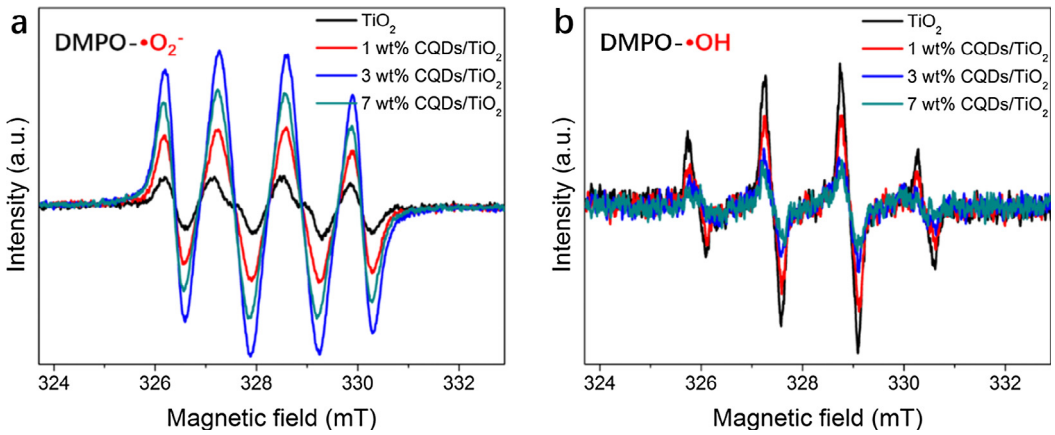

Fig. 6. DMPO spin-trapping ESR spectra of CQDs/TiO_2 composites with different CQDs content in (a) methanol dispersion and (b) aqueous dispersion under xenon lamp irradiation for 5 min.

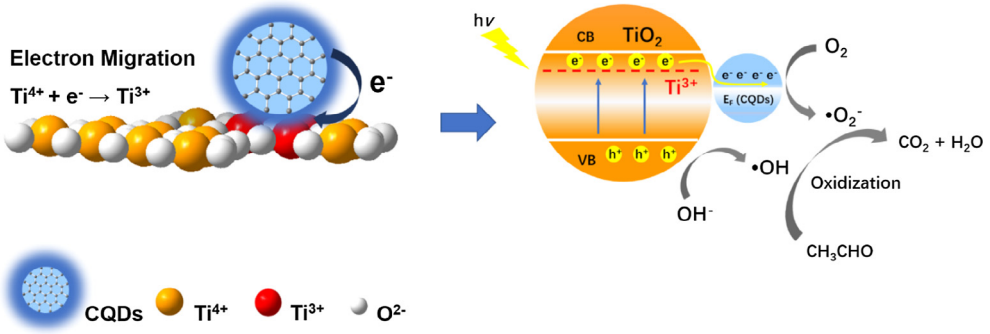

Fig. 7. Schematic illustration of the surface interaction between the heterostructured CQDs/TiO_2 composite and the corresponding photocatalytic mechanism.

3.6. Discussion on photocatalytic mechanism

Based on the aforementioned experiment results, the photodegradation ability for acetaldehyde of photocatalyst gets enhanced after modified with CQDs, and the possible photocatalytic mechanism of CQDs/TiO_2 composite is illustrated in Fig. 7.

In the CQDs/TiO_2 composite, the CQDs are grafted onto TiO_2 via Ti-O-C bond, and some delocalized electron of CQDs migrate to TiO_2 due to the work function difference, resulting in the generation of Ti^{3+} defects in TiO_2 matrix and positively charged surface environment of CQDs. On one hand, through electron interaction, Ti^{3+} ions could favor the O_2 adsorption on photocatalyst surface; on the other hand, with graphite-like electron structure and functional groups (Fig. 1c), the CQDs could promote the composites to adsorb organic compounds, improving the contact with target gas and further benefitting the photo-degradation process, especially for the gaseous indoor pollutant in low concentration. But excessive amount of CQDs attached to TiO_2 might lead to suppress the photocatalytic performance owing to reduced active sites on photocatalyst surface, and impeded migration of excessive adsorbed acetaldehyde.

After coupling with CQDs, the visible-light harvesting has been significantly improved in the modified TiO_2 photocatalyst. Understandably, the formation of Ti^{3+} donor energy level could narrow the band gap as Fig. 7 shown. Furthermore, through CQDs, some visible light could be harvested and upconverted to higher-energy photon for PCO excitation. In addition, the recombination of photo-generated electrons and holes in the CQDs/TiO_2 composite also get limited which is confirmed by the results of PL spectra and photocurrent response (Fig. 5c and 5d). Serving as remarkable electron reservoirs, the CQDs could harvest and stock photo-generated electron from conduction band of TiO_2, to hinder the recombination of electron-hole pairs and further facilitate the photocatalytic activity. Under light irradiation, the trapped photo-generated electrons on CQDs could further reduce the absorbed O_2 to reactive $\cdot O_2^-$, of which the production could depend on the photo-generated carrier separation efficiency and the amounts of photo-generated electron trapped by CQDs. Thus the enhanced electron-hole separation efficiency directly boosts the $\cdot O_2^-$ formation as substantiated in the DMPO spin-trapping ESR measurement (Fig. 6a).

4. Conclusion

In summary, the CQDs/TiO_2 heterostructured photocatalyst has been constructed and firstly applied to photodegrade flowing gaseous acetaldehyde under visible-light irradiation. Compared with the degradation efficiency 46% obtained by pristine TiO_2, the highest photodegradation efficiency 99% can be acquired based on the optimal photocatalytic performance of 3 wt% CQDs/TiO_2 under fluorescent lamp irradiation. And under visible-light irradiation, the 3 wt% CQDs/TiO_2 remained 30% removal efficiency while pristine TiO_2 showed no photocatalytic ability. The optimized photocatalytic performance of the composite could be ascribed to the conjoined CQDs for three aspects: (a) facilitating visible-light harvest by the formation of Ti^{3+} donor energy level and up-converted photoluminescence property of CQDs; (b) improving adsorption for

organic compounds due to the graphite-like electron structure and intrinsic functional groups of CQDs; (c) as an electron reservoir, inhibiting the recombining of photo-generated carriers and promoting the production of $\cdot O_2^-$. This work not only provides a heterostructured CQDs/TiO_2 composite material to efficiently photodegrade the flowing gaseous acetaldehyde, but also reveals some new functions of CQDs in the semiconductor-based photocatalytic mechanism. Since the CQDs/TiO_2 composite is capable of visible-light response with an enhanced photocatalytic ability for acetaldehyde removal, this promising composite photocatalyst could be expected as a qualified candidate for further indoor-air-purification applications.

Acknowledgment

This work was financially supported by the National Key Research and Development Program of China (2016YFA0203000), the International Partnership Program of Chinese Academy of Sciences (GJHZ1656), and the National Natural Science Foundation of China (No. 51702347).

Conflict of interest

The authors declare no competing financial interest.

Appendix A. Supplementary material

Supplementary data associated with this article can be found, in the online version, at https://doi.org/10.1016/j.apsusc.2018.01.104.

References

[1] S.B. Wang, H.M. Ang, M.O. Tade, Volatile organic compounds in indoor environment and photocatalytic oxidation: state of the art, Environ. Int. 33 (5) (2007) 694–705.
[2] N.E. Klepeis, W.C. Nelson, W.R. Ott, J.P. Robinson, A.M. Tsang, P. Switzer, et al., The National Human Activity Pattern Survey (NHAPS): a resource for assessing exposure to environmental pollutants, J. Expo Anal. Env. Epid. 11 (3) (2001) 231–252.
[3] J.D. Spengler, K. Sexton, Indoor air-pollution - a public-health perspective, Science 221 (4605) (1983) 9–17.
[4] C.S. Lee, F. Haghighat, W.S. Ghaly, A study on VOC source and sink behavior in porous building materials – analytical model development and assessment, Indoor Air 15 (3) (2005) 183–196.
[5] E. Uhde, T. Salthammer, Impact of reaction products from building materials and furnishings on indoor air quality - a review of recent advances in indoor chemistry, Atmos. Environ. 41 (15) (2007) 3111–3128.
[6] R. Lindahl, Aldehyde Dehydrogenases and Their Role in Carcinogenesis, Crit Rev Biochem Mol. 27 (4–5) (1992) 283–335.
[7] Y. Boyjoo, H.Q. Su, J. Liu, V.K. Pareek, S.B. Wang, A review on photocatalysis for air treatment: from catalyst development to reactor design, Chem. Eng. J. 310 (2017) 537–559.
[8] L.X. Zhong, J.J. Brancho, S. Batterman, B.M. Bartlett, C. Godwin, Experimental and modeling study of visible light responsive photocatalytic oxidation (PCO) materials for toluene degradation, Appl. Catal. B-Environ. 216 (2017) 122–132.
[9] M.N. Lyulyukin, P.A. Kolinko, D.S. Selishchev, D.V. Kozlov, Hygienic aspects of TiO_2-mediated photocatalytic oxidation of volatile organic compounds: air purification analysis using a total hazard index, Appl. Catal. B-Environ. 220 (2018) 386–396.
[10] A. Janczyk, E. Krakowska, G. Stochel, W. Macyk, Singlet oxygen photogeneration at surface modified titanium dioxide, J. Am. Chem. Soc. 128 (49) (2006) 15574–15575.
[11] D. Dvoranova, V. Brezova, M. Mazur, M.A. Malati, Investigations of metal-doped titanium dioxide photocatalysts, Appl. Catal. B-Environ. 37 (2) (2002) 91–105.
[12] X.B. Chen, C. Burda, The electronic origin of the visible-light absorption properties of C-, N- and S-doped TiO_2 nanomaterials, J. Am. Chem. Soc. 130 (15) (2008) 5018.
[13] L. Pan, J.J. Zou, X.W. Zhang, L. Wang, Water-mediated promotion of dye sensitization of TiO_2 under visible light, J. Am. Chem. Soc. 133 (26) (2011) 10000–10002.
[14] J.H. Yum, P. Walter, S. Huber, D. Rentsch, T. Geiger, F. Nuesch, et al., Efficient far red sensitization of nanocrystalline TiO_2 films by an unsymmetrical squaraine dye, J. Am. Chem. Soc. 129 (34) (2007) 10320.
[15] J.S. Luo, L. Ma, T.C. He, C.F. Ng, S.J. Wang, H.D. Sun, et al., TiO_2/(CdS, CdSe, CdSeS) nanorod heterostructures and photoelectrochemical properties, J. Phys. Chem. C. 116 (22) (2012) 11956–11963.
[16] W.J. Zhou, Z.Y. Yin, Y.P. Du, X. Huang, Z.Y. Zeng, Z.X. Fan, et al., Synthesis of few-layer MoS_2 nanosheet-coated TiO_2 nanobelt heterostructures for enhanced photocatalytic activities, Small 9 (1) (2013) 140–147.
[17] P. Peerakiatkhajohn, T. Butburee, J.H. Yun, H.J. Chen, R.M. Richards, L.Z. Wang, A hybrid photoelectrode with plasmonic Au@TiO_2 nanoparticles for enhanced photoelectrochemical water splitting, J Mater Chem A. 3 (40) (2015) 20127–20133.
[18] Y.F. Xu, C. Zhang, L.X. Zhang, X.H. Zhang, H.L. Yao, J.L. Shi, Pd-catalyzed instant hydrogenation of TiO_2 with enhanced photocatalytic performance, Energ. Environ. Sci. 9 (7) (2016) 2410–2417.
[19] A.Y. Chen, S.S. Shi, J.W. Wang, F. Liu, F. Wang, Y. Wang, et al., Microstructure and electrocatalytic performance of nanoporous gold foils decorated by TiO_2 coatings, Surf. Coat. Technol. 286 (2016) 113–118.
[20] H.J. Yu, Y.F. Zhao, C. Zhou, L. Shang, Y. Peng, Y.H. Cao, et al., Carbon quantum dots/TiO_2 composites for efficient photocatalytic hydrogen evolution, J. Mater. Chem. A. 2 (10) (2014) 3344–3351.
[21] J. Liu, Y. Liu, N.Y. Liu, Y.Z. Han, X. Zhang, H. Huang, et al., Metal-free efficient photocatalyst for stable visible water splitting via a two-electron pathway, Science. 347 (6225) (2015) 970–974.
[22] J. Wang, X. Zhang, J. Wu, H. Chen, S. Sun, J. Bao, et al., Preparation of Bi2S3/carbon quantum dot hybrid materials with enhanced photocatalytic properties under ultraviolet-, visible- and near infrared-irradiation, Nanoscale (2017).
[23] C. Zhu, C. Liu, Y. Zhou, Y. Fu, S. Guo, H. Li, et al., Carbon dots enhance the stability of CdS for visible-light-driven overall water splitting, Appl. Catal. B-Environ. 216 (2017) 114–121.
[24] G. Williams, B. Seger, P.V. Kamat, TiO_2-graphene nanocomposites. UV-assisted photocatalytic reduction of graphene oxide, Acs Nano 2 (7) (2008) 1487–1491.
[25] Y.J. Xu, Y.B. Zhuang, X.Z. Fu, New insight for enhanced photocatalytic activity of TiO_2 by doping carbon nanotubes: a case study on degradation of benzene and methyl orange, J. Phys. Chem. C 114 (6) (2010) 2669–2676.
[26] N. Zhang, Y.H. Zhang, M.Q. Yang, Z.R. Tang, Y.J. Xu, A critical and benchmark comparison on graphene-, carbon nanotube-, and fullerene-semiconductor nanocomposites as visible light photocatalysts for selective oxidation, J. Catal. 299 (2013) 210–221.
[27] H.B. Fu, T.G. Xu, S.B. Zhu, Y.F. Zhu, Photocorrosion inhibition and enhancement of photocatalytic activity for ZnO via hybridization with C-60, Environ. Sci. Technol. 42 (21) (2008) 8064–8069.
[28] R. Wang, K.Q. Lu, Z.R. Tang, Y.J. Xu, Recent progress in carbon quantum dots: synthesis, properties and applications in photocatalysis, J. Mater. Chem. A. 5 (8) (2017) 3717–3734.
[29] P. Chen, F.L. Wang, Z.F. Chen, Q.X. Zhang, Y.H. Su, L.Z. Shen, et al., Study on the photocatalytic mechanism and detoxicity of gemfibrozil by a sunlight-driven TiO_2/carbon dots photocatalyst: the significant roles of reactive oxygen species, Appl. Catal. B-Environ. 204 (2017) 250–259.
[30] A.L. Qu, H.L. Xie, X.M. Xu, Y.Y. Zhang, S.W. Wen, Y.F. Cui, High quantum yield graphene quantum dots decorated TiO_2 nanotubes for enhancing photocatalytic activity, Appl. Surf. Sci. 375 (2016) 230–241.
[31] J. Tian, Y.H. Leng, Z.H. Zhao, Y. Xia, Y.H. Sang, P. Hao, et al., Carbon quantum dots/hydrogenated TiO_2 nanobelt heterostructures and their broad spectrum photocatalytic properties under UV, visible, and near-infrared irradiation, Nano Energy 11 (2015) 419–427.
[32] S.L. Xie, H. Su, W.J. Wei, M.Y. Li, Y.X. Tong, Z.W. Mao, Remarkable photoelectrochemical performance of carbon dots sensitized TiO_2 under visible light irradiation, J. Mater. Chem. A. 2 (39) (2014) 16365–16368.
[33] S.N. Qu, X.Y. Wang, Q.P. Lu, X.Y. Liu, L.J. Wang, A biocompatible fluorescent ink based on water-soluble luminescent carbon nanodots, Angew. Chem. Int. Ed. 51 (49) (2012) 12215–12218.
[34] B. Siemensmeyer, J.W. Schultze, Xps and Ups studies of gas-phase oxidation, electrochemistry and corrosion behavior of Ti and Ti5ta, Surf. Interface Anal. 16 (1–12) (1990) 309–314.
[35] N.C. Saha, H.G. Tompkins, Titanium nitride oxidation chemistry - an X-ray photoelectron-spectroscopy study, J. Appl. Phys. 72 (7) (1992) 3072–3079.
[36] P. Babelon, A.S. Dequiedt, H. Mostefa-Sba, S. Bourgeois, P. Sibillot, M. Sacilotti, SEM and XPS studies of titanium dioxide thin films grown by MOCVD, Thin Solid Films 322 (1–2) (1998) 63–67.
[37] H. Irie, Y. Watanabe, K. Hashimoto, Carbon-doped anatase TiO_2 powders as a visible-light sensitive photocatalyst, Chem. Lett. 32 (8) (2003) 772–773.
[38] F. Zuo, L. Wang, T. Wu, Z.Y. Zhang, D. Borchardt, P.Y. Feng, Self-doped Ti^{3+} enhanced photocatalyst for hydrogen production under visible light, J Am Chem Soc. 132 (34) (2010) 11856–11857.
[39] W.Z. Fang, M.Y. Xing, J.L. Zhang, Modifications on reduced titanium dioxide photocatalysts: a review, J. Photochem. Photobiol. C 32 (2017) 21–39.
[40] F.B. Li, X.Z. Li, The enhancement of photodegradation efficiency using Pt-TiO_2 catalyst, Chemosphere 48 (10) (2002) 1103–1111.
[41] H. Tang, Y. Su, B. Zhang, A.F. Lee, M.A. Isaacs, K. Wilson, et al., Classical strong metal-support interactions between gold nanoparticles and titanium dioxide, Sci. Adv. 3 (10) (2017), e1700231-e.
[42] J. Ke, X.Y. Li, Q.D. Zhao, B.J. Liu, S.M. Liu, S.B. Wang, Upconversion carbon quantum dots as visible light responsive component for efficient enhancement of photocatalytic performance, J. Colloid Interf Sci. 496 (2017) 425–433.
[43] H. Idriss, K.S. Kim, M.A. Barteau, Carbon-carbon bond formation via aldolization of acetaldehyde on single crystal and polycrystalline TiO_2 surfaces, J. Catal. 139 (1) (1993) 119–133.

[44] Y. Nosaka, A.Y. Nosaka, Generation and detection of reactive oxygen species in photocatalysis, Chem. Rev. 117 (17) (2017) 11302–11336.
[45] H.C. Zhang, H. Huang, H. Ming, H.T. Li, L.L. Zhang, Y. Liu, et al., Carbon quantum dots/Ag_3PO_4 complex photocatalysts with enhanced photocatalytic activity and stability under visible light, J. Mater. Chem. 22 (21) (2012) 10501–10506.
[46] B.E. Salisbury, W.T. Wallace, R.L. Whetten, Low-temperature activation of molecular oxygen by gold clusters: a stoichiometric process correlated to electron affinity, Chem. Phys. 262 (1) (2000) 131–141.
[47] K. Komaguchi, T. Maruoka, H. Nakano, I. Imae, Y. Ooyama, Y. Harima, Electron-transfer reaction of oxygen species on TiO_2 nanoparticles induced by sub-band-gap illumination, J. Phys. Chem. C 114 (2) (2010) 1240–1245.